PHYSICAL REVIEW B

CONDENSED MATTER

THIRD SERIES, VOLUME 31, NUMBER 1 1 JANUARY 1985

Dependence of EPR in diluted magnetic semiconductors on the host lattice

R. E. Kremer* and J. K. Furdyna
Physics Department, Purdue University, West Lafayette, Indiana 47907
(Received 13 March 1984)

We have studied the EPR in six wide-gap diluted magnetic semiconductors: $Cd_{1-x}Mn_xTe$, $Cd_{1-x}Mn_xSe$, $Cd_{1-x}Mn_xS$, $Zn_{1-x}Mn_xTe$, $Zn_{1-x}Mn_xSe$, and $Zn_{1-x}Mn_xS$, all containing about 10 at. % Mn, in order to determine the extent to which the EPR of the magnetic ions depends on their environment in these materials. The EPR linewidth and intensity as a function of temperature was obtained by measuring Faraday rotation and ellipticity associated with the resonance, a technique suitable for EPR studies when the resonance is very broad. It was found that, although the behavior of the Mn^{2+} EPR is qualitatively the same in all the above materials, its intensity and linewidth show a striking and systematic dependence on the nonmagnetic host lattice. Specifically, for a given group-VI element (anion) the resonance becomes broader and weaker as the atomic number of the group-II element (nonmagnetic cation) decreases; but, in contrast, for a given cation the resonance becomes broader and weaker as the atomic number of the anion *increases*. This provides interesting insights into the nature of the interaction between Mn^{2+} ions in diluted magnetic semiconductors.

I. INTRODUCTION

Diluted magnetic semiconductors (DMS) are semiconducting alloys whose crystal lattice is made up in part of substitutional magnetic ions. To a great extent, such materials studied so far are II-VI compounds, where a fraction of the group-II ions has been replaced by Mn^{2+}, e.g., $Cd_{1-x}Mn_xTe$ and $Zn_{1-x}Mn_xSe$. Among many interesting features,[1] these materials display important magnetic properties (e.g., spin-glass transition at low temperatures) that are not yet fully understood.[2-5]

One important magnetic property persistently occurring in all DMS is a very pronounced *increase* of the EPR linewidth observed with decreasing temperature and/or increasing Mn concentration.[3,6] Although the microscopic details of this low-temperature broadening have not yet been theoretically formulated, it is clear that this linewidth behavior must depend intimately on the physics of the inter-Mn interaction. Systematic studies of the EPR in these materials should therefore contribute significantly to the understanding of the mechanisms underlying the magnetic properties of DMS in general.

The purpose of this paper is to present experimental evidence that, for a given Mn concentration and temperature, the EPR linewidth and intensity in DMS depend strongly on the host lattice, which in turn suggests that the Mn-Mn interaction depends strongly on the nonmagnetic environment. The correlations observed between the EPR linewidth and the properties of the nonmagnetic host atoms offer several insights into the factors governing this Mn-Mn interaction.

II. EXPERIMENT

The measurements were carried out on six members of the $(II\text{-}VI)_{1-x}(Mn\text{-}VI)_x$ family of DMS: $Zn_{1-x}Mn_xS$, $Zn_{1-x}Mn_xSe$, $Zn_{1-x}Mn_xTe$, $Cd_{1-x}Mn_xS$, $Cd_{1-x}Mn_xSe$, and $Cd_{1-x}Mn_xTe$, all with $x \approx 0.1$. The samples were prepared either by Bridgman growth or by sintering. The materials have either the zinc-blende or the wurtzite structure. The nominal Mn concentrations, methods of preparation, and crystal structures of the samples are listed in Table I. All compounds in the present investigation are wide-gap semiconductors ($E_g > 1.6$ eV). We have purposely not included in this study the narrow-gap, Hg-based DMS (e.g., $Hg_{1-x}Mn_xTe$, $E_g \approx 0.1$ at $x = 0.1$) to avoid complications in the interpretation of EPR due to the presence of free carriers.

The dynamic magnetic susceptibility associated with EPR has been investigated at 35 GHz by measuring the microwave Faraday effect (rotation and ellipticity) due to EPR. This transmission technique, described elsewhere in detail,[6,7] has been developed to circumvent the difficulties in EPR measurements arising from the extremely broad resonance lines, which occur in DMS at low temperatures. Briefly, the experimental arrangement is basically a microwave analog of an optical transmission apparatus for studying Faraday rotation. The waves travel in a cylindri-

TABLE I. Key properties of DMS samples studied.

Material	Nominal x	Crystal structure	NN cation separation	Preparation
$Cd_{1-x}Mn_xTe$	0.10	zinc blende	4.57 Å	Bridgman
$Cd_{1-x}Mn_xSe$	0.085	wurtzite	4.28 Å	Bridgman
$Cd_{1-x}Mn_xS$	0.10	wurtzite	4.12 Å	Bridgman
$Zn_{1-x}Mn_xTe$	0.10	zinc blende	4.33 Å	Bridgman
$Zn_{1-x}Mn_xSe$	0.10	zinc blende	4.02 Å	sintering
$Zn_{1-x}Mn_xS$	0.12	wurtzite	3.84 Å	sintering

cal waveguide, axially along the bore of a superconducting solenoid. The samples are located at the center of the magnet and are in powder form, filling completely the cross section of the guide, typically to a thickness of 3 to 5 mm. The waves incident on the sample are linearly polarized. The waveguide is terminated by a linear polarizer and detector, which together act as the analyzer. The angle between the analyzer and the incident plane of polarization can be varied by means of a rotating joint. The technique is capable of measuring angles smaller than 1′ of arc, and Faraday ellipticities (ratio of minor-to-major axes of the transmitted elliptically polarized wave pattern) down to about 10^{-4}.

As described earlier,[6,7] the Faraday rotation θ_F and ellipticity ϵ_F provide a measure of the real and the imaginary part of the dynamic magnetic susceptibility

$$\theta_F=\tfrac{1}{4}\frac{\omega d\sqrt{\kappa}}{c}\mathrm{Re}(\chi_- -\chi_+)\approx -\tfrac{1}{4}\frac{\omega d\sqrt{\kappa}}{c}\mathrm{Re}\chi_+ , \quad (1)$$

$$\epsilon_F=\tfrac{1}{4}\frac{\omega d\sqrt{\kappa}}{c}\mathrm{Im}(\chi_- -\chi_+)\approx -\tfrac{1}{4}\frac{\omega d\sqrt{\kappa}}{c}\mathrm{Im}\chi_+ , \quad (2)$$

where ω is the angular frequency, d is the sample thickness, c is the speed of light, κ is the lattice dielectric constant of the DMS crystal, and χ_+ and χ_- are the dynamic magnetic susceptibilities corresponding to the two senses of circular polarization about the dc magnetic field $\vec{B}$. In terms of the Bloch model, $\chi_\pm$ have the familiar form

$$\chi_\pm=\mp\chi_0\frac{\omega_L(\omega\mp\omega_L)T_2^2}{1+(\omega\mp\omega_L)^2T_2^2}\pm i\chi_0\frac{\omega_L T_2}{1+(\omega\mp\omega_L)^2T_2^2} , \quad (3)$$

where χ_0 is the dc magnetic susceptibility, T_2 is the spin-spin relaxation time, and $\omega_L=geB/2m$ is the Larmor frequency, g being the g factor of the Mn^{2+} ions. In the above, χ_+ corresponds to the EPR-active polarization. When $\omega T_2>1$, $\chi_+ \gg \chi_-$. Under these conditions the final forms of Eqs. (1) and (2) become valid, so that θ_F and ϵ_F are seen to provide a direct measure of the real and imaginary parts of the EPR-active dynamic magnetic susceptibilities, respectively.

Since all materials investigated are wide-gap semiconductors, free-carrier contributions to the Faraday effect need not be considered. Finally, since the samples used in this investigation are in powder form, we define an *effective* thickness

$$d_{\mathrm{eff}}=M/(DA) , \quad (4)$$

where M is the total mass of the powder, D is the density of the sample, and A is the cross-sectional area of the cylindrical waveguide. This quantity corresponds to the thickness which the same amount of material would have if it were a solid slab filling the waveguide. Although not important for line-*shape* considerations, this standardization of sample thickness is necessary to permit comparison between EPR *intensities* observed on different powder samples.

III. RESULTS AND DISCUSSION

Figure 1 shows the Faraday rotation and ellipticity observed at 4.2 K for four of the compounds studied. The values measured were normalized to 1-cm effective thickness to permit comparison between samples. Note that the magnitudes of the Faraday rotation (which provide the measure of $\mathrm{Re}\chi_+$) and the Faraday ellipticity (which measures $\mathrm{Im}\chi_+$) are much larger for the sulfides than for

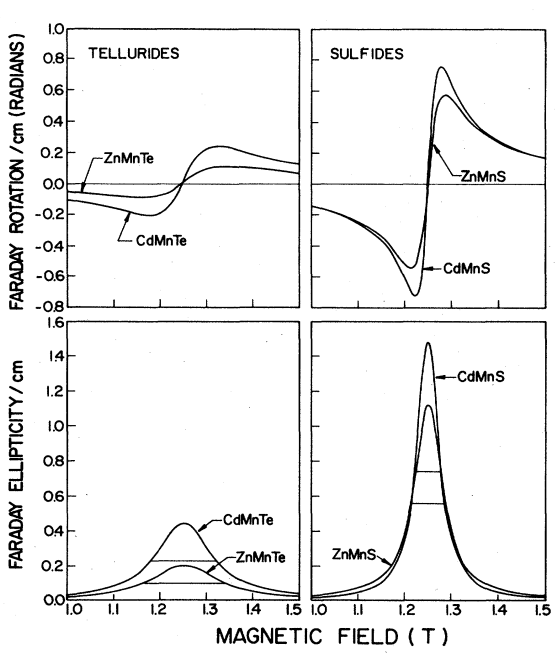

FIG. 1. Microwave Faraday rotation θ_F and Faraday ellipticity ϵ_F in DMS powders near EPR, obtained at 35 GHz and 4.2 K for four DMS with approximately 10 at. % Mn. The data are normalized to unit effective thickness to permit quantitative comparison between different samples. The full width at half-height for the ϵ_F data is indicated by a horizontal line and is nearly identical to the peak-to-peak separation in the θ_F data. Note that Cd-based DMS show stronger and narrower EPR than their Zn-based counterparts.

the tellurides. Also note that, for a given chalcogen, the Cd compounds give a stronger signal than the Zn compounds. The selenides (not shown in this figure, to avoid crowding) lie between the S and Te compounds, with CdMnSe again showing a stronger and narrower resonance than the ZnMnSe. To facilitate comparison of resonance widths, a horizontal bar is drawn across each ellipticity curve at half-height, indicating full width at half height (FWHH). As can be seen at a glance, the stronger resonances are also narrower, without conserving the area under the curve, i.e., the narrower the resonance, the larger the *integrated* resonance intensity.

To better display the relative dependence of the EPR intensity and linewidth on the chalcogen, we have also displayed the data for the Zn and Cd compounds separately in Fig. 2. Again the trend is very clear: For the same Mn concentration, the sulfides manifest the greatest integrated intensities and narrowest lines, with tellurides at the other extreme and selenides in between. An apparent exception in Fig. 2 is the linewidth of $Cd_{1-x}Mn_xSe$, which is approximately the same as that for $Cd_{1-x}Mn_xS$. Note, however, that the $Cd_{1-x}Mn_xSe$ available for this investigation had $x=0.085$, less than the sulfide (see Table I). A sample with $x=0.1$ would display a broader line,[3] thus preserving the same linewidth sequence as seen in the Zn-based DMS.

The study of EPR as a function of temperature in these six DMS compounds indicates that, while the resonance narrows as the temperature increases, the relative behavior of the resonance intensity and linewidth, illustrated in Figs. 1 and 2 for 4.2 K, persists over the entire range covered in this investigation ($2<T<100$ K). The variation of the linewidth with temperature for the six compounds is shown in Fig. 3. Again we remark that the $Cd_{1-x}Mn_xSe$ data correspond to $x=0.085$. For $x=0.1$ the corresponding curve in Fig. 3 would be shifted upward relative to the $Cd_{1-x}Mn_xS$ results.

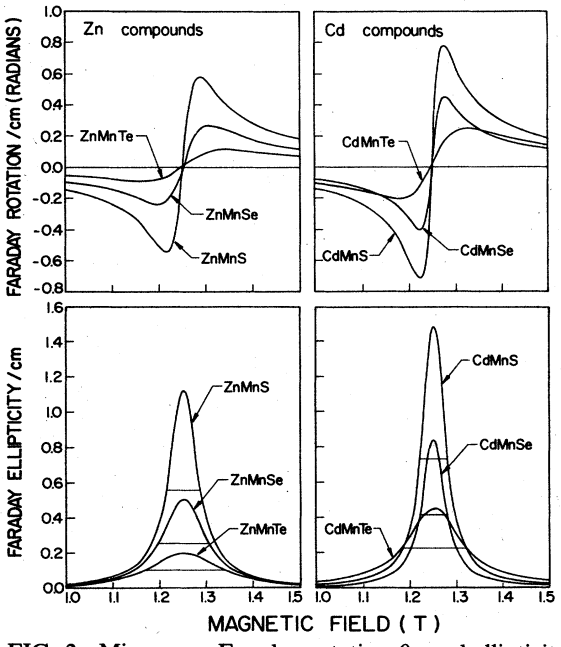

FIG. 2. Microwave Faraday rotation θ_F and ellipticity ϵ_F at 35 GHz and 4.2 K, showing EPR in six DMS compounds with approximately 10 at. % Mn (see Table I). The values of θ_F and ϵ_F are normalized to unit effective thickness ($d_{\text{eff}}=1$ cm) to permit comparison between samples. The full width at half-height is indicated by a horizontal line in the ϵ_F curves. Note the progression of integrated intensities and linewidths with the size of the anion. Note also that the $Cd_{1-x}Mn_xSe$ data are for $x=0.085$. For $x=0.10$ the line would be about 20% wider (Ref. 3).

Before proceeding to the implications of the data presented above, it is important to recall two pertinent features already established in earlier experiments on DMS. In previous EPR studies it has been found[3] that, at any one temperature and for a given host lattice, the EPR linewidth in DMS becomes broader as the Mn concentration increases. Although the specific nature of the mechanism which leads to this broadening has not yet been identified, clearly the broadening is caused by some interaction between the Mn^{2+} ions which increases as the system of Mn^{2+} ions becomes more dense. We also know from earlier magnetization measurements[8] that, as the Mn concentration is increased in DMS, the magnetic moment per Mn^{2+} ion decreases due to antiferromagnetic interaction (such as pairing) between the Mn^{2+} ions. Thus, with increasing Mn concentration (or, equivalently, with increasing overlap between the Mn^{2+} wave functions), the contribution *per ion* to χ_0—and thus to the integrated EPR intensity—would be expected to decrease at any one temperature.

In the case of the present data we have already noted that, when the EPR for any two samples is compared, the narrower line systematically corresponds to a larger *integrated* intensity (area under ϵ_F, which in turn is proportional to χ_0), as can be seen at a glance by comparing, e.g., the data for the Zn compounds in Fig. 2. On the basis of the preceding comments we know that the line will broaden, and χ_0 will decrease, with increasing degree of Mn-Mn interaction. We can therefore conclude that, for a given anion (S, Se, or Te), the inter-ion interaction is systematically weaker in the Cd compounds than in the

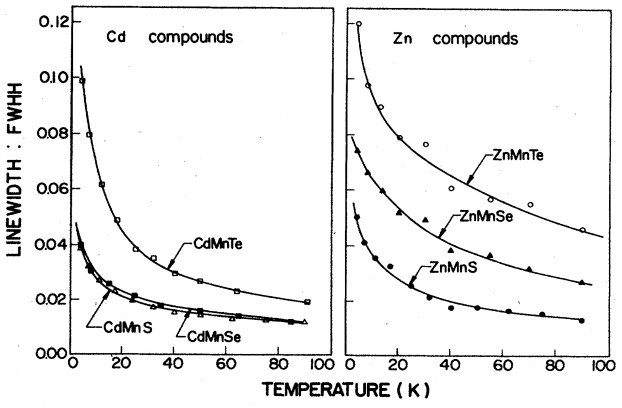

FIG. 3. Temperature dependence of the EPR full width at half-height (in tesla) for Cd-based and Zn-based DMS (shown separately for clarity). The $Cd_{1-x}Mn_xSe$ data correspond to $x=0.085$. For $x=0.10$ the $Cd_{1-x}Mn_xSe$ would be somewhat (approximately 15—20 %) higher.

Zn compounds (i.e., the interaction decreases with increasing atomic number of the cation). And, for a given cation (Cd or Zn), the strength of the interaction decreases with *decreasing* atomic number of the anion.

It is tempting to interpret the observed difference between the Cd and Zn compounds simply in terms of the lattice parameters. In Table I we have listed the nearest-neighbor (NN) separation in the respective fcc and hcp sublattice (i.e., the closest possible separation for a pair of Mn ions in the zinc-blende and wurtzite structures). This parameter (corresponding to $a/\sqrt{2}$ for zinc-blende structures and to the lattice parameter "a" in wurtzite structures) is obtained by interpolation between the value for the nonmagnetic II-VI crystal (e.g., CdSe) and that for the corresponding Mn-VI compound (in this case, the wurtzite phase of MnSe).[9,10] We thus note from Table I that, for any anion, the NN separation in the cation sublattice is always smaller for the Zn compounds than for Cd, suggesting a larger overlap—and thus a stronger interaction—in the former group of compounds. Similar arguments have already been invoked in comparing the magnetic phase diagrams of Zn- and Cd-based DMS with higher Mn concentration, the spin-glass temperatures being consistently higher in the Zn compounds, indicating that the Mn-Mn interaction increases with decreasing Mn-Mn separation.[5,11]

We see, however, that the case is altogether different when we compare the EPR results for different anions, keeping the cation the same: the resonances are broader and weaker—and thus the Mn-Mn interaction is greater—for the heavier anions, even though the NN separation also increases with the anion atomic number, as shown in the table. We are therefore forced to conclude that the nature of the anion itself is important in determining the degree of Mn-Mn interaction. It is thus tempting to suggest that the anion plays a major role in mediating the Mn-Mn interaction in DMS.

It must be pointed out that in the argument used above we have been making comparisons between *all* the DMS compounds investigated, without regard to whether they form zinc-blende or wurtzite crystals. This is perfectly valid in the context involving short-range interactions. In both the zinc-blende and the wurtzite environment, a given cation (or anion) has the same number of nearest neighbors in its respective fcc or hcp sublattice, and each cation (e.g., each Mn^{2+}) is surrounded by a chalcogen tetrad which is identical in both structures. The important parameters determining the Mn-Mn interaction therefore must be the nearest-neighbor distance and the type of ion surrounding the Mn^{2+} sites. In this respect both crystal structures can be regarded as identical, permitting direct comparison between zinc-blende and wurtzite compounds.

Thus the results reported in this paper, although qualitative, strongly suggest that—for a given anion—the degree of Mn-Mn interaction decreases with increasing lattice parameter, i.e., with the physical separation between the Mn ions, as should perhaps be expected. On the other hand, these results also indicate that the interaction increases with increasing size of the intervening anions between the Mn neighbors (i.e., it is much stronger in tellurides than in sulfides). Although these qualitative conclusions appear plausible, it would be important to extend these studies systematically to a wider range of compositions of DMS—including Hg compounds—in order to obtain a deeper understanding of the Mn-Mn interaction in DMS, and hopefully to put this understanding on a quantitative footing.

ACKNOWLEDGMENTS

The authors wish to thank Professor W. Giriat for some of the specimens used in this investigation. The support of the National Science Foundation, Materials Research Laboratory Program, Grant No. DMR 80-20249, is also gratefully acknowledged.

*Present address: Oregon Graduate Center, Beaverton, Oregon 97006.

[1]J. K. Furdyna, J. Appl. Phys. **53**, 7637 (1982).
[2]R. R. Galazka, S. Nagata, and P. H. Keesom, Phys. Rev. B **22**, 3344 (1980).
[3]S. B. Oseroff, Phys. Rev. B **25**, 6584 (1982).
[4]M. Escorne and A. Mauger, Phys. Rev. B **25**, 4674 (1982).
[5]S. P. McAlister, J. K. Furdyna, and W. Giriat, Phys. Rev. B **29**, 1310 (1984).
[6]R. E. Kremer and J. K. Furdyna, J. Magn. Magn. Mater. **40**, 185 (1983).
[7]R. E. Kremer, Ph.D. dissertation, Purdue University, 1983 (unpublished).
[8]See, e.g., J. A. Gaj, R. Planel, and G. Fishman, Solid State Commun. **29**, 435 (1979).
[9]A. Pajaczkowska, Prog. Cryst. Growth Charact. **1**, 289 (1978).
[10]J. K. Furdyna, W. Giriat, D. F. Mitchell, and G. I. Sproule, J. Solid State Chem. **46**, 349 (1983).
[11]Y. Q. Yang, P. H. Keesom, J. K. Furdyna, and W. Giriat, J. Solid State Chem. **49**, 20 (1983).